

# Fluctuations in models of biological macroevolution

Per Arne Rikvold\*

*School of Computational Science, Center for Materials Research and Technology,  
National High Magnetic Field Laboratory, and Department of Physics  
Florida State University, Tallahassee, FL 32306, USA*

Fluctuations in diversity and extinction sizes are discussed and compared for two different, individual-based models of biological coevolution. Both models display power-law distributions for various quantities of evolutionary interest, such as the lifetimes of individual species, the quiet periods between evolutionary upheavals larger than a given cutoff, and the sizes of extinction events. Time series of the diversity and measures of the size of extinctions give rise to flicker noise. Surprisingly, the power-law behaviors of the probability densities of quiet periods in the two models differ, while the distributions of the lifetimes of individual species are the same.

## I. INTRODUCTION

Biological evolution presents many problems concerning highly nonlinear, nonequilibrium systems of interacting entities that are well suited for study by methods from statistical mechanics. An excellent review of this rapidly growing field is found in Ref. 1. Among these problems are those concerned with *coevolution*: the simultaneous evolution of many species, whose mutual interactions produce a constantly changing *fitness landscape*. Throughout this process, new species are created and old species go extinct. A question that is still debated in evolutionary biology is whether evolution on the macroscale proceeds gradually or in ‘fits and starts,’ as suggested by Eldredge and Gould.<sup>2,3,4</sup> In the latter mode, known as *punctuated equilibria*, species and communities appear to remain largely unchanged for long periods of time, interrupted by brief (on a geological timescale) periods of mass extinctions and rapid change.

A coevolution process involves a large range of timescales, from the ecologically relevant scales of a few generations, to geological scales of millions or billions of generations. Traditionally, models of macroevolution have been constructed on a highly coarse-grained timescale. (The best-known such model to physicists is probably the Bak-Sneppen model.<sup>5</sup>) However, the long-time dynamics of the evolution is clearly driven by ecological processes, mutations, and selection at comparatively short timescales. As a result, in recent years several new models have been proposed that are designed to span the disparate ecological and evolutionary timescales. These models include the Webworld model,<sup>6,7,8</sup> the Tangled-nature model,<sup>9,10</sup> and simplified versions of the latter.<sup>11,12,13</sup> In this paper I discuss and compare some of the properties of fluctuations in two simplified coevolution models: the model introduced in Ref. 11 and a different model that I am currently developing.<sup>14</sup>

The rest of this paper is organized as follows. In Sec. II I introduce the two models, in Sec. III I compare and discuss numerical results from large-scale Monte Carlo simulations for the different models, and in Sec. IV I present a summary and conclusions.

## II. MODELS

Both of the models studied here consider haploid species whose genome is represented by a bit string of length  $L$ , so that there are a total of  $2^L$  potential species, labeled by an index  $I \in [0, 2^L - 1]$ . At the end of each generation, an individual of species  $I$  can with probability  $P_I$  give rise to  $F$  offspring and then die, or with probability  $(1 - P_I)$  it dies without offspring. The fecundity  $F$  is assumed fixed and will be chosen appropriately for each model as discussed below. During its birth, an offspring individual may undergo mutation with a small probability  $\mu/L$  per bit in its genome. During a mutation event, a bit in the genome is flipped, and the mutated offspring individual is considered as belonging to a different species than its parent.

The reproduction probability  $P_I(t)$  of species  $I$  in generation  $t$  depends on the interactions of individuals of that species with other species,  $J$ , that are present in the community with nonzero populations  $n_J$ , as well as possibly on its ability to utilize an external resource,  $R$ . It is given by the convenient nonlinear form,

$$P_I(t) = \frac{1}{1 + \exp[\Phi_I(R, \{n_J\})]}, \quad (1)$$

which resembles the acceptance probability in a Monte Carlo simulation using Glauber transition rates.<sup>15</sup> The function  $\Phi_I$  depends linearly on the set of all nonzero populations in generation  $t$ ,  $\{n_J(t)\}$ , and possibly also on the external

resource  $R$ . When  $\Phi_I$  is large and negative, the reproduction probability is near unity, while large positive values lead to a low reproduction probability. The coupling to the  $n_J$  is effected via the interaction matrix  $\mathbf{M}$ , whose elements  $M_{IJ}$  are chosen randomly (with restrictions discussed below for the individual models) from a uniform distribution on  $[-1, +1]$ . If  $M_{IJ} > 0$  and  $M_{JI} < 0$ , species  $I$  is a predator and  $J$  its prey, or *vice versa*, while  $M_{IJ}$  and  $M_{JI}$  both positive denotes mutualism or symbiosis, and both negative denote competition. Once  $\mathbf{M}$  is chosen at the beginning of a simulation, it remains fixed (“quenched randomness”). These interactions (together with other, model-specific parameters) determine whether or not a species will have a sufficient reproduction probability to be successful *in a particular community* of other species. Typically, only a small subset of species have nonzero populations at any one time, forming a community.

**Model A:**

In Model A, which was introduced and studied in Refs. 11,12,13,  $\Phi_I$  takes the form

$$\Phi_I^A(\{n_J(t)\}) = - \sum_J M_{IJ} n_J(t) / N_{\text{tot}}(t) + N_{\text{tot}}(t) / N_0, \quad (2)$$

where  $N_{\text{tot}}(t) = \sum_J n_J(t)$  is the total population at  $t$ . In this model, the Verhulst factor  $N_0$  prevents the population from indefinite growth and can be seen as representing an environmental “carrying capacity.”<sup>16</sup> The interaction matrix has elements that are randomly distributed over  $[-1, +1]$ , except that  $M_{II} = 0$  to focus on the effects of interspecies interactions. Here, Model A will be simulated with the following parameter values:  $F = 4$  (see below),  $N_0 = 2000$ , and  $\mu = 10^{-3}$ .

**Model B:**

The new Model B is a predator/prey model. It is somewhat more realistic than Model A in that the population is maintained by a subset of the species that can utilize the external resource  $R$  (primary producers, or autotrophs). Other species can maintain themselves only by predation on one or more of the producer species (consumers, or heterotrophs). These modifications lead to the restrictions that the off-diagonal part of  $\mathbf{M}$  must be antisymmetric, and further that if  $I$  is a producer and  $J$  a consumer, then  $I$  must be the prey of  $J$ , so that  $M_{IJ} < 0$ . To avoid runaway population growth, the diagonal elements are chosen randomly on  $[-1, 0)$ . Such negative self interactions are commonly used in population dynamics models.<sup>17</sup> The specific form of  $\Phi_I$  in this model is

$$\Phi_I^B(R, \{n_J(t)\}) = b_I - R\eta_I / N_{\text{tot}}(t) - \sum_J M_{IJ} n_J(t) / N_{\text{tot}}(t), \quad (3)$$

where  $b_I > 0$  can be seen as a “cost of reproduction,” and  $\eta_I > 0$  is the coupling to the external resource. The latter is positive for producers and zero for consumers. In this implementation of the model, both  $b_I$  and the nonzero  $\eta_I$  are chosen uniformly from  $(0, 1]$  at the beginning of the simulation and kept fixed thereafter. Here, Model B will be simulated with the following parameter values:  $F = 2$  (see below),  $R = 2000$ , and  $\mu = 10^{-3}$ . Only 5% of the potential species are producers (i.e., have  $\eta_I > 0$ ), and in order to obtain food webs with more realistic connectivity, 90% of the  $M_{IJ}/M_{JI}$  pairs are randomly chosen to be zero, giving a *connectance*<sup>18,19,20,21,22,23</sup> of 10%, while the elements of the nonzero pairs are chosen on  $[-1, +1]$  as described above.

Both models are sufficiently simple that the populations and stabilities of fixed-point communities can be obtained analytically for zero mutation rate. These analytical results are extensively compared with simulations in Refs. 11,12, and 14. For the purposes of the present study I just mention that the analytical stability results yield intervals for the fecundity  $F$ , inside which it is ensured that a fixed-point community in the absence of mutations is stable toward small deviations in all directions. The values of  $F$  used here are chosen to yield such stable fixed-point communities for both models.

My focus in this paper is to compare the fluctuations and long-time correlations in the two models for quantities of significance in ecology and evolutionary biology. One such quantity is the *diversity* of a community. This quantity is defined in many ways in the literature, most simply as the total number of species that exist with nonzero populations at a given time (also known as the *species richness*).<sup>24</sup> Here I define it as  $D(t) = \exp[S(\{n_I(t)\})]$ , where  $S$  is the information-theoretical entropy<sup>25,26</sup>,

$$S(\{n_I(t)\}) = - \sum_{\{I|\rho_I(t)>0\}} \rho_I(t) \ln \rho_I(t) \quad (4)$$

with  $\rho_I(t) = n_I(t) / N_{\text{tot}}(t)$ . This definition of diversity has the advantage that it is weighted away from species with very small populations, which in these models are likely to be short-lived, unsuccessful mutants. In ecology it is known as the Shannon-Wiener index.<sup>24</sup> It is expected to exhibit a low noise level during periods with little apparent evolutionary turnover (periods of *stasis*<sup>2,3,4</sup>), while it should fluctuate much more strongly during highly active periods, such as mass extinctions or the emergence of new major species. Other quantities that can be monitored, and are expected to give similar information, are the number of species that go extinct in a single generation, either by itself, or weighted by the maximum population attained by the species that go extinct.

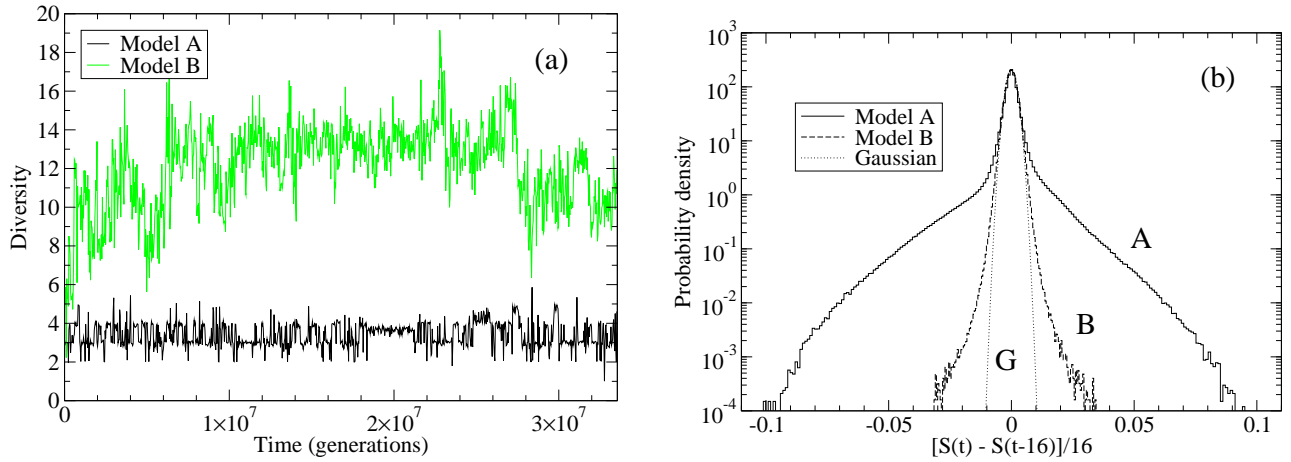


FIG. 1: **(a)**: Typical diversity time series of  $T = 2^{25} = 33\,554\,432$  generations from Model A (black) and Model B (gray, green online). To facilitate printing, the data are sampled only every  $2^{15} = 32\,768$  generations, corresponding roughly to the graphical resolution of the figure. While this somewhat reduces the apparent range of the fluctuations, the general shape of the time series is preserved. **(b)**: Histograms representing the probability density of the logarithmic derivative of the diversity,  $dS(t)/dt$ . The data were averaged over 16 generations in each run, and then averaged over 16 independent runs for Model A (solid, marked A) and 12 runs for Model B (dashed, marked B). The central parts of both histograms are well fitted by *the same* Gaussian distribution (dotted, marked G).

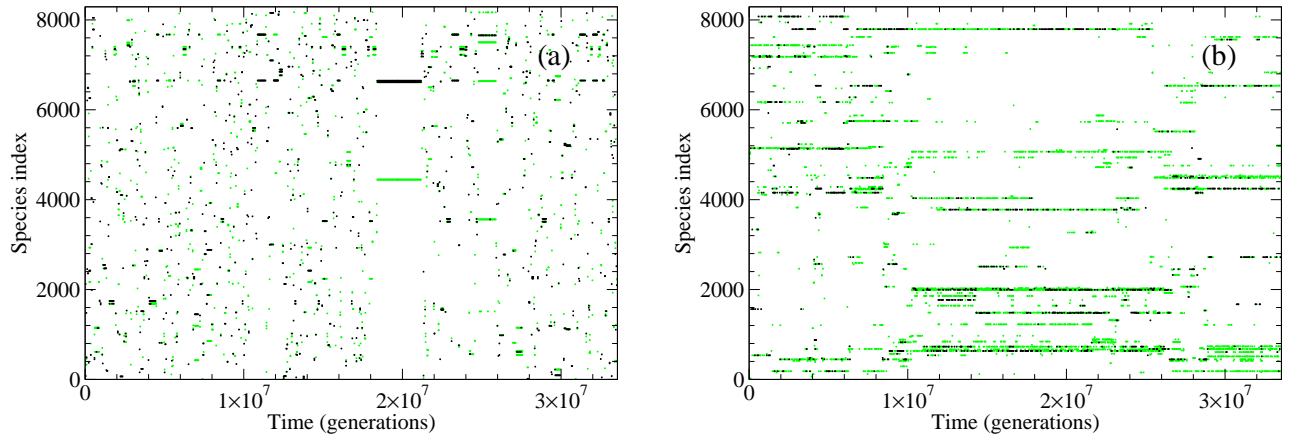


FIG. 2: Graphic representation of the community structure vs time, showing only species with populations between 101 and 1000 (gray, green online) and above 1000 (black). See discussion in the text. **(a)**: Model A. Data for the same simulation run illustrated in Fig. 1(a). **(b)**: Model B. Data for the same simulation run illustrated in Fig. 1(a). For ease of plotting, only every other data point is shown.

### III. NUMERICAL RESULTS AND ANALYSIS

Both models were simulated for  $T = 2^{25} = 33\,554\,432$  generations, and several of their statistical properties were compared. Figure 1(a) contains time series for representative simulation runs for both models. The diversity of Model A is significantly less than for Model B, but both models show periods during which the relative fluctuations are modest (quiet periods), separated by shorter periods during which the diversity changes strongly. Histograms of the logarithmic derivative of the diversity,  $dS(t)/dt$ , are shown in Fig. 1(b). In both models the probability densities have Gaussian central peaks of very nearly the same width, with “heavy wings.” While the Gaussian peak represents fluctuations due to the stochastic population dynamics<sup>12</sup> and the creation and extinction of small populations of unsuccessful mutants, the wings represent large changes in the composition of the communities. This can be seen

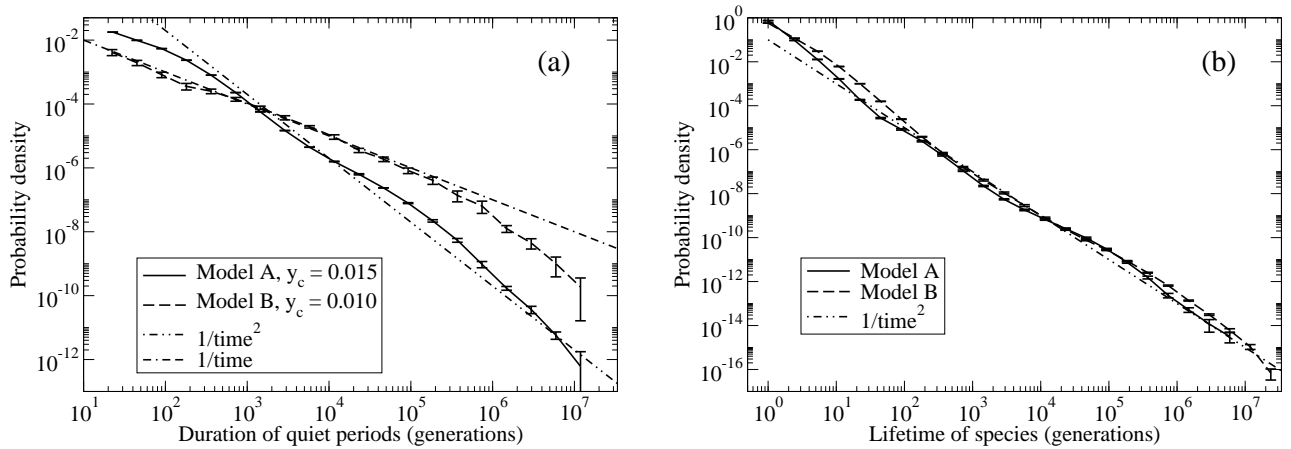


FIG. 3: **(a)**: Log-log plot of histograms representing the probability density of the durations of quiet periods, estimated as the periods between times when  $y = |dS(t)/dt|$  (averaged over 16 generations) exceeds a cutoff  $y_c$ . For Model A (solid) and Model B (dashed). Results for Model A were averaged over 16 runs, and for Model B over 12 runs. The error bars are standard errors, based on the spread between runs. The two dot-dashed straight lines represent  $1/t^2$  and  $1/t$  power laws, respectively. **(b)**: Log-log plot of histograms representing the probability density of the lifetimes of individual species for Model A (solid) and Model B (dashed). Results for Model A were averaged over 8 runs, and for Model B over 12 runs. The error bars were obtained as in part (a). The dot-dashed straight line represents a  $1/t^2$  power law.

clearly by comparing the timing of the diversity fluctuations in Fig. 1 with Fig. 2, which shows the populations of individual species versus time for the same simulation runs shown in Fig. 1. Quiet periods can be identified as periods between times when  $|dS(t)/dt|$  exceeds a given threshold. However, the durations of the quiet periods so defined clearly depend on the magnitude of the threshold (discussed further below) and the functional form of the wings. Histograms representing the probability densities for the durations of quiet periods for both models are shown together in Fig. 3(a). Both histograms display approximate power-law behavior over at least five decades, but, somewhat surprisingly, the powers are significantly different: approximately  $1/\text{time}^2$  for Model A and  $1/\text{time}$  for Model B. In contrast, the probability densities of the lifetimes of individual species (the time from the population of a species becomes nonzero until it again vanishes) are very close for the two models, both closely following a  $1/\text{time}^2$  power law over more than six decades (see Fig. 3(b)). I believe this discrepancy between the distributions of the durations of quiet periods and the lifetimes of individual species is related to the fact that extinction events are much more highly synchronized in Model A than in Model B. This can be clearly seen from the time evolution of the community structure of the two models, shown in Fig. 2. In Model A all the major species in a community usually go extinct within a relatively short period of time, linking the duration of a quiet period closely to the lifetimes of its major constituent species. As a result, both the lifetime and quiet-period distributions for Model A show approximate  $1/\text{time}^2$  behavior. Conversely, extinctions in Model B tend to trigger further extinctions of only a part of the total food web that describes the community, producing a much weaker synchronization between individual extinctions and the duration of relatively quiet periods. This ability of the food web to avoid global collapse triggered by the extinction of a single species may be the cause of the wide  $1/\text{time}$  distribution of quiet periods in this model. However, the  $1/\text{time}$  distribution does not appear to be a direct consequence of the low connectance of the interactions for this model: tests of Model B with a connectance of 100% and 10% potential producers also resulted in a duration distribution with approximate  $1/\text{time}$  decay.

The time series for  $|dS(t)/dt|$  is highly intermittent, and while the quiet periods are power-law distributed in both models, individual active periods, during which the activity remains continuously above the cutoff threshold, are generally exponentially distributed with a mean of just a few generations, except for very small thresholds. This was discussed for Model A in Ref. 11, and I find the situation to be the same for Model B.

An analysis method that is less dependent on the details of the distribution of the large fluctuations and the choice of cutoff, is the power spectral density (PSD) of a time series of a suitable global activity measure. It may be reasonable to consider both models as examples of *extremal dynamics*, in which the least “stable” parts of the system “collapse,” leading to avalanches of readjustments throughout the system. It is known for such systems<sup>27</sup> that if the probability density of the times between these local events has the long-time power-law dependence  $\sim 1/t^{\tau_1}$  with  $\tau_1 \leq 2$ , then the PSD of the global activity will depend on frequency as  $1/f^\alpha$ , where  $\alpha = \tau_1 - 1$  (with a hard-to detect logarithmic correction if  $\tau_1 = 2$ ).<sup>28</sup> In the systems considered here, it seems reasonable to identify these local waiting times with

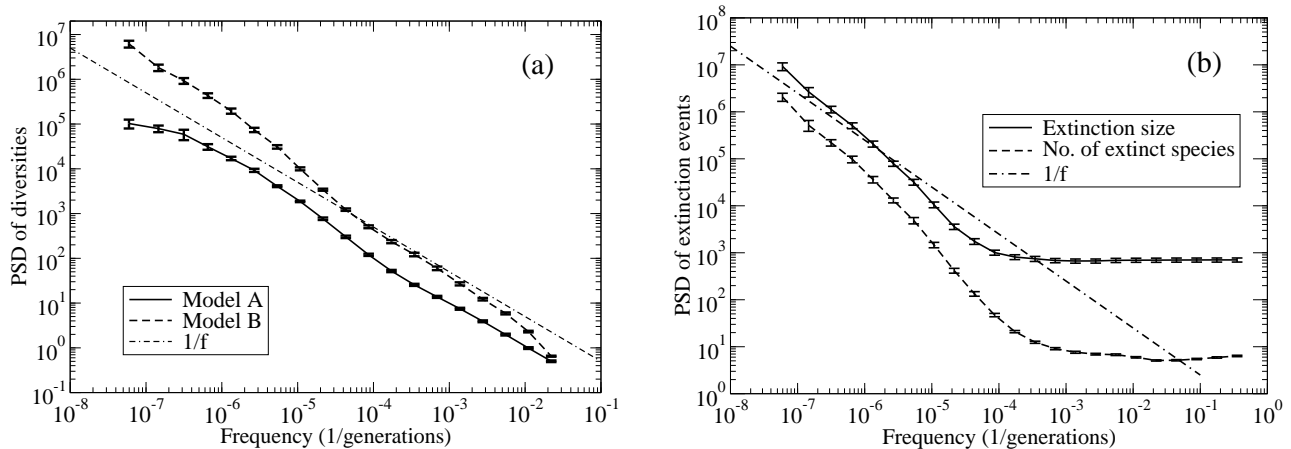


FIG. 4: **(a)**: Log-log plot of octave-averaged power spectral densities (PSD) for the diversity  $D(t)$  for Model A (solid) and Model B (dashed). The straight, dot-dashed line is a guide to the eye, corresponding to  $1/f$  behavior. The data were averaged over 16 independent runs for Model A and 12 runs for Model B, and the error bars are standard errors based on the differences between independent runs. **(b)**: Log-log plot of octave-averaged PSDs for the number of species going extinct in one generation (dashed) and for the number of species going extinct, weighted by the maximum population attained by each species, or *extinction size* (solid). Both PSDs refer to Model B and are averages over 12 independent runs. The straight, dot-dashed line corresponds to  $1/f$  behavior, and error bars were calculated as in part (a).

the lifetimes of individual species, such that  $\tau_1 \approx 2$  for both models. This reasoning then predicts that the PSD of the diversity in both cases should exhibit practically pure  $1/f$  noise (i.e.,  $\alpha \approx 1$ ). Indeed, the PSDs for both models, which are shown in Fig. 4(a), exhibit  $1/f$  like behavior over many decades. Except for a difference in their overall magnitudes, the two PSDs behave essentially alike for frequencies between  $10^{-6}$  and  $10^{-2}$  generations $^{-1}$ . For the very lowest frequencies, the PSD for Model A appears to level off, but the amount of data in this regime is small, and much longer simulations would be needed to accurately determine the PSDs below  $10^{-6}$  generations $^{-1}$ . Power-law distributions and PSDs that fall off as  $1/f^\alpha$  with  $\alpha \approx 1$  have been obtained from the fossil record.<sup>29</sup> However, such power-law behaviors have only been observed over one or two decades in time or frequency, and there are arguments to the effect that  $1/f$  spectra extracted in Ref. 29 may be severely influenced by the analysis method.<sup>30</sup>

Another quantity that can be used to determine the severity of an extinction event is the total number of species that go extinct in a single generation. However, this quantity is heavily influenced by the repeated extinctions of small populations of unsuccessful mutants of species with large populations. A better measure might therefore be the number of species that go extinct, weighted by the maximum population attained by each species during its lifetime. For convenience I shall call this latter measure the *extinction size*. It can be seen as a rough measure of the maximum fitness attained by the species that go extinct in a particular generation. PSDs of both quantities for Model B are shown in Fig. 4(b). Like the diversity PSDs, both these PSDs show  $1/f$  like behavior for low frequencies. However, they also have a wide region of near-white noise for higher frequencies.

In models governed by extremal dynamics, the exponents  $\alpha$  for the frequency dependence of the PSD,  $\tau_1$  for the duration of local events (here interpreted as the lifetimes of individual species), and  $\tau$  for the duration of quiet periods where the activity measure (here  $|dS(t)/dt|$ ) falls below some cutoff  $y_c$ , are connected by the following scaling relations:<sup>27</sup>

$$\begin{aligned}
 \alpha &= 1 - \mu \\
 \tau_1 &= 2 - \mu \\
 \tau &= 1 + \mu - \sigma,
 \end{aligned}
 \tag{5}$$

where  $\mu$  and  $\sigma$  are two independent exponents that depend on the spatial dimensionality  $d$  of the underlying model and both vanish in the limit  $d \rightarrow 0$ .<sup>31</sup> One thus notes that (assuming that my identification of the quantities measured in the models studied here with quantities in the extremal-dynamics systems is valid) the exponents  $\alpha = 1$ ,  $\tau_1 = 2$ , and  $\tau = 1$ , observed for Model B, coincide with those of a zero-dimensional extremal-dynamics system. On the other hand, Model A does not seem to fit into this pattern. It remains a question for further study to decide how appropriate this analysis is.

As seen in Fig. 3(a), the probability density of the duration  $s$  of quiet periods in Model B is well described as  $p(s) \sim s^{-\tau}$  with  $\tau \approx 1$ , multiplied by a function that approaches zero for large  $s$  and a constant for small  $s$ .

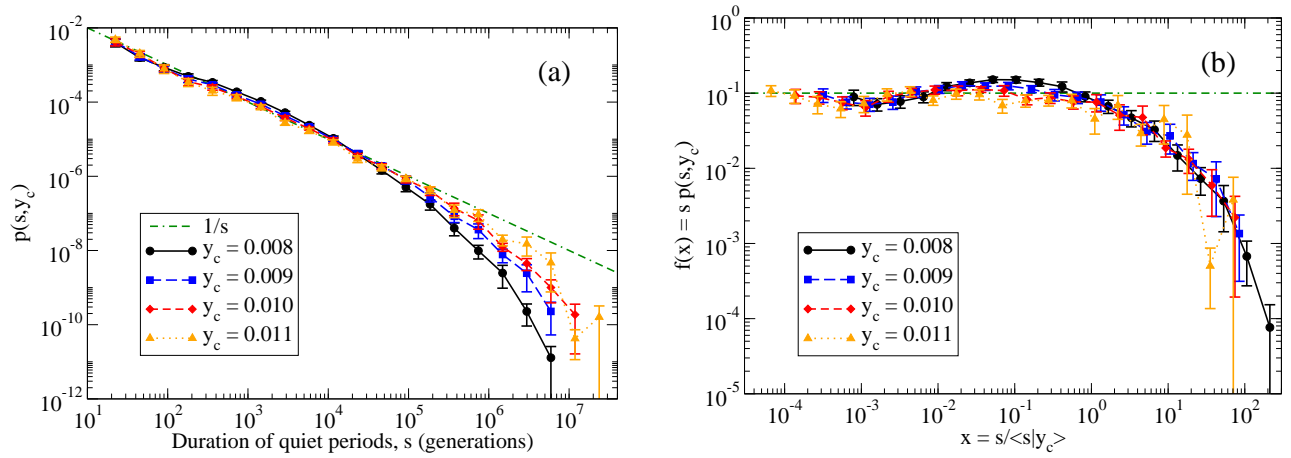


FIG. 5: **(a)**: Log-log plots of histograms representing the probability density  $p(s, y_c)$  of the duration  $s$  of quiet periods for Model B, as obtained with different values of the cutoff  $y_c$ . The dot-dashed straight line corresponds to  $1/s$  power-law behavior. **(b)**: Log-log plot of the scaling function  $f(x) = s p(s, y_c)$  vs the scaling variable  $x = s / \langle s | y_c \rangle$ .

Figure 5(a) shows that this function depends on the cutoff  $y_c$ , and it is naturally expressed as a scaling function,

$$p(s, y_c) = s^{-\tau} f(s/g(y_c)) . \quad (6)$$

The mean value of  $s$  as calculated from the numerical  $p(s, y_c)$ ,  $\langle s | y_c \rangle$ , would seem a natural choice for  $g(y_c)$ , as long as it is much less than the total time  $T$  of the simulation. Thus, the argument of the scaling function would be  $x = s / \langle s | y_c \rangle$ . In the relatively narrow range of the four values of  $y_c$  used in Fig. 5(a),  $\langle s | y_c \rangle$  is well approximated by the power law  $\langle s | y_c \rangle = 27948 (y_c / 0.008)^\gamma$  with  $\gamma \approx 7.84$ , and the scaling function,

$$f(x) = s^\tau p(s, y_c) = x^\tau \langle s | y_c \rangle^{\tau-1} \langle s | y_c \rangle p(x \langle s | y_c \rangle, y_c) \equiv x^\tau \langle s | y_c \rangle^{\tau-1} \tilde{p}(x) . \quad (7)$$

The resulting  $f(x)$  is shown in Fig. 5(b) for  $\tau = 1$ . The data collapse is reasonable, but it is not very sensitive to the value of  $\gamma$ , which can be reduced to near 5 without giving a significantly inferior collapse.

#### IV. CONCLUSION

In this paper I have discussed the fluctuations in two different, simplified models of biological macroevolution that both are based on the birth/death behavior of single individuals on the ecological timescale. On evolutionary timescales both models give rise to power-law distributions of characteristic waiting times and power spectra that exhibit  $1/f$  like flicker noise, in agreement with some interpretations of the fossil record.<sup>29,30</sup> The main difference in the construction of the models is that in Model A the population size is controlled by a Verhulst factor, while in Model B the population is maintained by a small percentage of the species that have the ability to directly utilize an external resource (producers or autotrophs). All other species must maintain themselves as predators (consumers or heterotrophs). In both models the probability density of the lifetimes of individual species follows a  $1/\text{time}^2$  power law and, consistently, the power spectra of the time series of diversity and extinction sizes show  $1/f$  noise. However, the probability density of quiet periods, defined as the times between events when the magnitude of the logarithmic derivative of the diversity exceeds a given cutoff, behaves differently in the two models. In Model B, the quiet-period distribution goes as  $1/\text{time}$ , consistent with the universality class of the zero-dimensional Bak-Sneppen model. In contrast, in Model A the behavior is proportional to  $1/\text{time}^2$ , like the lifetimes of individual species. The difference between the behaviors can be linked to the lower degree of synchronization between extinction events in Model B. It remains a topic for further research to see whether this difference extends to more realistic modifications of Model B.

#### Acknowledgments

I thank R. K. P. Zia for a pleasant and fruitful collaboration in formulating and studying Model A, V. Sevim for the data on Model A that appear in Fig. 3(b), and J. W. Lee for useful discussions.

This work was supported in part by the U.S. National Science Foundation through Grants No. DMR-0240078 and DMR-0444051, and by Florida State University through the School of Computational Science, the Center for Materials Research and Technology, and the National High Magnetic Field Laboratory.

- 
- \* Electronic address: rikvold@csit.fsu.edu
- <sup>1</sup> B. Drossel, “Biological evolution and statistical physics,” *Adv. Phys.* **50**, pp. 209–295, 2001.
  - <sup>2</sup> N. Eldredge and S. J. Gould, “Punctuated equilibria: An alternative to phyletic gradualism,” in *Models In Paleobiology*, T. J. M. Schopf, ed., pp. 82–115, Freeman, Cooper, San Francisco, 1972.
  - <sup>3</sup> S. J. Gould and N. Eldredge, “Punctuated equilibria: The tempo and mode of evolution reconsidered,” *Paleobiology* **3**, pp. 115–151, 1977.
  - <sup>4</sup> S. J. Gould and N. Eldredge, “Punctuated equilibrium comes of age,” *Nature (London)* **366**, pp. 223–227, 1993.
  - <sup>5</sup> P. Bak and K. Sneppen, “Punctuated equilibrium and criticality in a simple model of evolution,” *Phys. Rev. Lett.* **71**, pp. 4083–4086, 1993.
  - <sup>6</sup> G. Caldarelli, P. G. Higgs, and A. J. McKane, “Modelling coevolution in multispecies communities,” *J. theor. Biol.* **193**, pp. 345–358, 1998.
  - <sup>7</sup> B. Drossel, P. G. Higgs, and A. J. McKane, “The influence of predator-prey population dynamics on the long-term evolution of food web structure,” *J. theor. Biol.* **208**, pp. 91–107, 2001.
  - <sup>8</sup> B. Drossel, A. McKane, and C. Quince, “The impact of non-linear functional responses on the long-term evolution of food web structure,” *J. theor. Biol.* **229**, pp. 539–548, 2004.
  - <sup>9</sup> M. Hall, K. Christensen, S. A. di Collobiano, and H. J. Jensen, “Time-dependent extinction rate and species abundance in a tangled-nature model of biological evolution,” *Phys. Rev. E* **66**, Art. No. 011904, 2002.
  - <sup>10</sup> K. Christensen, S. A. di Collobiano, M. Hall, and H. J. Jensen, “Tangled-nature: A model of evolutionary ecology,” *J. theor. Biol.* **216**, pp. 73–84, 2002.
  - <sup>11</sup> P. A. Rikvold and R. K. P. Zia, “Punctuated equilibria and  $1/f$  noise in a biological coevolution model with individual-based dynamics,” *Phys. Rev. E* **68**, Art. No. 031913, 2003.
  - <sup>12</sup> R. K. P. Zia and P. A. Rikvold, “Fluctuations and correlations in an individual-based model of biological coevolution,” *J. Phys. A* **37**, pp. 5135–5155, 2004.
  - <sup>13</sup> V. Sevim and P. A. Rikvold, “A biological coevolution model with correlated individual-based dynamics,” in *Computer Simulation Studies in Condensed Matter Physics XVII*, D. P. Landau, S. P. Lewis, and H.-B. Schüttler, eds., Springer-Verlag, Berlin, in press. E-print arXiv:q-bio.PE/0403042.
  - <sup>14</sup> P. A. Rikvold, in preparation.
  - <sup>15</sup> D. P. Landau and K. Binder, *A Guide to Monte Carlo Simulations in Statistical Physics*, Cambridge University Press, Cambridge, 2000.
  - <sup>16</sup> P. F. Verhulst, “Notice sur la loi que la population suit dans son accroissement,” *Corres. Math. et Physique* **10**, pp. 113–121, 1838.
  - <sup>17</sup> J. D. Murray, *Mathematical Biology*, Springer-Verlag, Berlin, 1989.
  - <sup>18</sup> M. R. Gardner and W. R. Ashby, “Connectance of large dynamic (cybernetic) systems: Critical values for stability,” *Nature (London)* **228**, pp. 784–784, 1970.
  - <sup>19</sup> R. M. May, “Will a large complex system be stable?,” *Nature (London)* **238**, pp. 413–414, 1972.
  - <sup>20</sup> P. Yodzis, “The connectance of real ecosystems,” *Nature (London)* **284**, pp. 544–545, 1980.
  - <sup>21</sup> J. Dunne, R. J. Williams, and N. D. Martinez, “Network structure and diversity loss in food webs: Robustness increases with connectance,” *Ecol. Lett.* **5**, pp. 558–567, 2002.
  - <sup>22</sup> D. Garlaschelli, G. Caldarelli, and L. Pietronero, “Universal scaling relations in food webs,” *Nature (London)* **423**, pp. 165–168, 2003.
  - <sup>23</sup> D. Garlaschelli, “Universality in food webs,” *Eur. Phys. J. B* **38**, pp. 277–285, 2004.
  - <sup>24</sup> C. J. Krebs, *Ecological Methodology*, Harper & Row, New York, 1989. Chap. 10.
  - <sup>25</sup> C. E. Shannon, “A mathematical theory of communication,” *Bell Syst. Tech. J.* **27**, pp. 379–423, 628–656, 1948.
  - <sup>26</sup> C. E. Shannon and W. Weaver, *The Mathematical Theory of Communication*, University of Illinois Press, Urbana, 1949.
  - <sup>27</sup> M. Paczuski, S. Maslov, and P. Bak, “Avalanche dynamics in evolution, growth, and depinning models,” *Phys. Rev. E* **53**, pp. 414–443, 1996.
  - <sup>28</sup> I. Procaccia and H. Schuster, “Functional renormalization-group study of universal  $1/f$  noise,” *Phys. Rev. A* **28**, pp. 1210–1212, 1983.
  - <sup>29</sup> R. V. Solé, S. C. Manrubia, M. Benton, and P. Bak, “Self-similarity of extinction statistics in the fossil record,” *Nature (London)* **388**, pp. 764–767, 1997.
  - <sup>30</sup> M. E. J. Newman and G. J. Eble, “Power spectra and extinction in the fossil record,” *Proc. R. Soc. Lond. B* **266**, pp. 1267–1270, 1999.
  - <sup>31</sup> S. N. Dorogovtsev, J. F. F. Mendes, and Y. G. Pogorelov, “Bak-Sneppen model near zero dimension,” *Phys. Rev. E* **62**, pp. 295–298, 2000.